Asymmetric flux tube

M. G. Olsson and Siniša Veseli
Department of Physics, University of Wisconsin, Madison, Wisconsin 53706
(Received 16 September 1994)

We consider a relativistic flux tube with arbitrary mass spinless quarks at the ends. In the unequal-mass case the additional constraint that the center of momentum is fixed must be included. An analytic classical circular solution is found and is used as a correspondence limit. The quantized equations for mesons at rest are constructed and solved. A comparison is made with all available spin-averaged heavy-light and heavy-heavy states. We find evidence for running of the heavy quark masses as well as the short range coupling constant.

PACS number(s): 12.39.−x

I. INTRODUCTION

The relativistic flux tube (RFT) model shows promise to provide a realistic description of all meson states. The RFT model is in essence a description of dynamical confinement [1–4]. For slowly moving quarks rigorous QCD relativistic corrections [5–7] clearly demonstrate that the scalar confinement potential picture is incorrect [2, 7]. On the other hand, the RFT dynamics are consistent with both spin-dependent [3, 8, 9] and spin-independent [2, 3] QCD expectations. The basic assumption of the RFT model is that the QCD dynamical ground state for large quark separation consists of a rigid straight tubelike color flux configuration connecting the quarks. In this idealized limit the quarks and tube are shown in Fig. 1. Although based on a simple physical picture this model follows directly from the QCD Lagrangian with natural approximations to the Wilson action [10].

The heavy-light mesons are important for many reasons. For our present purposes, these mesons exhibit relativistic dynamics while still maintaining some simplifying aspects. The heavy quark mass suppresses most spin dependence so that a spinless quark analysis has considerable validity. The one heavy quark also means the reduced Salpeter equation [11] will be appropriate and that a relative time degree of freedom is unimportant.

In the present work we have focused on the following points.

(1) The extension to unequal quark masses requires the solution of several technical problems. These problems have their origin in locating the center of momentum and ensuring that the total momentum of the meson vanishes.

(2) The classical solution for rotational motion with unequal quark masses provides a useful check on our quantum solution. We have obtained an analytic solution which satisfies the requirement that the total meson momentum is zero.

(3) Both spinless and fermionic quark analyses share a common orbital angular momentum analysis. The techniques developed here will therefore be of direct utility in the more realistic calculation.

(4) Because of the suppressed spin dependence due to the small color magnetic moment of the heavy quark, a spin-averaged analysis is realistic.

(5) We reconsider the question of the symmetrization of operators in the quantized RFT equations. Algorithms are developed for finding the symmetrical perpendicular velocity operators.

(6) We have considered all the spin-averaged heavy-heavy and heavy-light states and found the expected *runnning* of the heavy quark masses, as well as the short-range interaction, follows in a natural way.

As established previously [1–4] the classical angular momentum of two quarks plus two tube segments joined at the c.m. is

$$J = W_{r_1}\gamma_{\perp_1} v_{\perp_1} r_1 + 2ar_1^2 f(v_{\perp_1}) + (1 \to 2) \ , \tag{1}$$

where

$$W_{r_i} = \sqrt{p_{r_i}^2 + m_i^2} \ , \tag{2}$$

$$4v_\perp f(v_\perp) = \frac{\arcsin v_\perp}{v_\perp} - \gamma_\perp^{-1} \ , \tag{3}$$

$$\gamma_\perp^{-2} = 1 - v_\perp^2 \ . \tag{4}$$

The classical Hamiltonian for this system is

$$H = W_{r_1}\gamma_{\perp_1} + ar_1 \frac{\arcsin v_{\perp_1}}{v_{\perp_1}} + (1 \to 2) \ . \tag{5}$$

For unequal-mass quarks additional conditions [3] must be imposed so that the meson c.m. is at rest. These conditions are

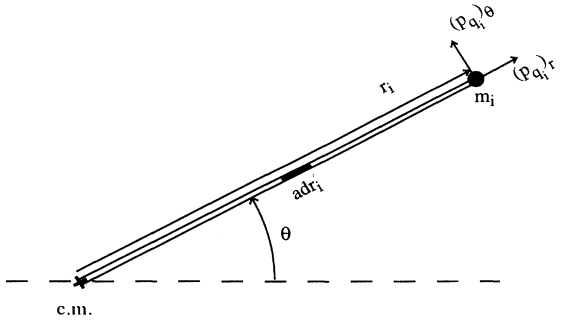

FIG. 1. Portion of a meson consisting of a segment of flux tube from the center of momentum to the ith quark.

$$p_{r_1} = p_{r_2} \equiv p_r \ , \tag{6}$$

$$P_\perp = 0 = W_{r_1}\gamma_{\perp_1}v_{\perp_1} + a\frac{r_1}{v_{\perp_1}}(1-\gamma_{\perp_1}^{-1}) - (1\to 2) \ . \tag{7}$$

Finally, the straight flux tube condition is

$$\frac{v_{\perp_1}}{r_1} = \frac{v_{\perp_2}}{r_2} \ . \tag{8}$$

For equal-mass quarks the $P_\perp$ condition (7) is satisfied since $v_{\perp_1} = v_{\perp_2}$. For heavy-light mesons where $m_2 \gg m_1$ and also $m_2 \gg ar_1$, the $P_\perp$ condition can be satisfied with $v_{\perp_2} \simeq 0$ (i.e., the c.m. point is coincident with the heavy quark). For all other (asymmetrical) mesons all of the above relations (1)–(8) must be used in the construction of the solution. This aspect is the central problem addressed here.

In Sec. II we consider the purely rotational classical solutions to the RFT equations. These results will provide a useful correspondence check on the quantum solution. Section III formulates the quantized RFT equations and their solutions are discussed in Sec. IV. In Sec. V we test the model by comparing it to all observed spin-averaged masses of mesons containing one or two heavy quarks. We observe that better global agreement with the data is obtained if the heavy quark masses run with QCD scale. Our conclusions are summarized in Sec. VI.

II. CLASSICAL (YRAST) SOLUTION

The classical solution of the RFT equations having minimum energy for a given angular momentum (the *yrast* solution) corresponds to circular motion, i.e., $p_r = 0$. In this case the RFT equations (1) and (5) become

$$J = m_1\gamma_{\perp_1}v_{\perp_1}r_1 + 2ar_1^2 f(v_{\perp_1}) + (1\to 2) \ , \tag{9}$$

$$H = m_1\gamma_{\perp_1} + ar_1\frac{\arcsin v_{\perp_1}}{v_{\perp_1}} + (1\to 2) \ . \tag{10}$$

The condition (7) that the c.m. momentum vanishes becomes

$$P_\perp = 0 = m_1\gamma_{\perp_1}v_{\perp_1} + a\frac{r_1}{v_{\perp_1}}(1-\gamma_{\perp_1}^{-1}) - (1\to 2) \ . \tag{11}$$

Along with the straight tube condition (8), the above three relations can be used to find the yrast solution $M = H(J)$.

A shortcut to the yrast solution directly uses the circular dynamical condition. In the Lagrangian approach [1, 12] the radial derivative of the Lagrangian must vanish since $\dot{p}_r = 0$. Another way to obtain the same result is to consider the force on the ith quark in two reference systems. In its rest frame the quark experiences a force $-a\hat{\mathbf{r}}_i$ due to the tube. In the c.m. rest frame, where the quark is moving with the velocity $v_\perp$ perpendicular to the tube, the transverse force is $a/\gamma_{\perp_i}$ and for circular orbits this must equal the mass $m_i\gamma_{\perp_i}$ times the centripetal acceleration or

$$(m_i\gamma_{\perp i})\frac{v_{\perp_i}^2}{r_i} = \frac{a}{\gamma_{\perp_i}} \ . \tag{12}$$

This, along with the straight string condition (8), assures that the meson is at rest [i.e., the total linear momentum (11) vanishes]. From (12) we also have

$$v_{\perp_i}^2 = \frac{ar_i}{m_i + ar_i} \ , \tag{13}$$

$$\gamma_{\perp_i}^2 = 1 + \frac{ar_i}{m_i} \ . \tag{14}$$

The total interquark distance is evidently

$$r = r_1 + r_2 \ , \tag{15}$$

and using (8) and (13), we obtain

$$r_1 = \frac{m_2 + ar}{m_1 + m_2 + 2ar} \ , \tag{16}$$

$$r_2 = \frac{m_1 + ar}{m_1 + m_2 + 2ar} \ . \tag{17}$$

When the above expressions are substituted back into (13) and (14), we find

$$v_{\perp_1}^2 = \frac{ar(m_2 + ar)}{(m_1 + ar)(m_1 + m_2 + ar)} \ , \tag{18}$$

$$v_{\perp_2}^2 = \frac{ar(m_1 + ar)}{(m_2 + ar)(m_1 + m_2 + ar)} \ , \tag{19}$$

$$\gamma_{\perp_i}^2 = \frac{(m_i + ar)(m_1 + m_2 + ar)}{m_i(m_1 + m_2 + 2ar)} \ . \tag{20}$$

The quantities r_i, $v_{\perp_i}$, and $\gamma_{\perp_i}$ have now been expressed in terms of the interquark distance r. The circular RFT equations can similarly be expressed in terms of r. Equation (9) for the meson angular momentum becomes

$$2\frac{J}{r} = \frac{\sqrt{ar}}{(m_1 + m_2 + 2ar)^{\frac{3}{2}}}\left[\sqrt{m_1}(m_2 + ar)^{\frac{3}{2}} + \sqrt{m_2}(m_1 + ar)^{\frac{3}{2}}\right] + \frac{(m_1 + m_2 + ar)(m_1 + ar)(m_2 + ar)}{(m_1 + m_2 + 2ar)^2}\left[\arcsin v_{\perp_1} + \arcsin v_{\perp_2}\right] \ , \tag{21}$$

and the state mass M from (10) is

$$M=\sqrt{\frac{m_1+m_2+ar}{m_1+m_2+2ar}}\left[\sqrt{m_1(m_1+ar)}+\sqrt{m_2(m_2+ar)}\right]$$
$$+\frac{\sqrt{ar(m_1+m_2+ar)(m_1+ar)(m_2+ar)}}{m_1+m_2+2ar}\left[\arcsin v_{\perp_1}+\arcsin v_{\perp_2}\right]\ . \tag{22}$$

In (21) and (22), $v_{\perp_1}$ and $v_{\perp_2}$ are functions of r given by (18) and (19). The above circular solutions reduce to the equal-mass case considered earlier [12].

Now we can easily establish three limiting cases.

A. Heavy-heavy case ($m_1, m_2 \gg ar$)

Equations (21) and (22) can be expanded in the small quantities $\frac{ar}{m_1}$ and $\frac{ar}{m_2}$ with the results

$$J^2=\left(\frac{m_1m_2a}{m_1+m_2}\right)r^3\ , \tag{23}$$
$$M=m_1+m_2+\frac{3}{2}ar\ . \tag{24}$$

From the above the shifted Regge slope is

$$\frac{dJ}{d(M-m_1-m_2)^2}=\left(\frac{m_1m_2}{m_1+m_2}\right)^{\frac{2}{3}}\frac{J^{-\frac{1}{3}}}{3a^{\frac{4}{3}}}\ . \tag{25}$$

B. Heavy-light case ($m_1 = 0, m_2 \gg ar$)

Again, from (21) and (22) in this limit we find

$$J=\frac{\pi ar^2}{4}\ , \tag{26}$$
$$M=m_2+\frac{\pi ar}{2}\ . \tag{27}$$

Eliminating r the shifted Regge slope is

$$\frac{J}{(M-m_2)^2}=\frac{1}{\pi a}\ . \tag{28}$$

C. Light-light case ($m_1 = m_2 = 0$)

For zero-mass quarks the tube carries all the rotational momentum and energy of the meson. In this limit we obtain

$$J=\frac{\pi ar^2}{8}\ , \tag{29}$$
$$M=\frac{\pi ar}{2}\ , \tag{30}$$

giving a Regge slope (Nambu) of

$$\frac{J}{M^2}=\frac{1}{2\pi a}\ . \tag{31}$$

The various limiting situations are illustrated in Figs. 2 and 3. We choose $m_2 = 1.5$ GeV, $a = (2\pi)^{-1}$ GeV^2 and plot the shifted Regge slope as a function of J. In Fig. 2 we take $m_1 = 0$. The solid curve shows a shifted slope of two units at small J as expected from the heavy-

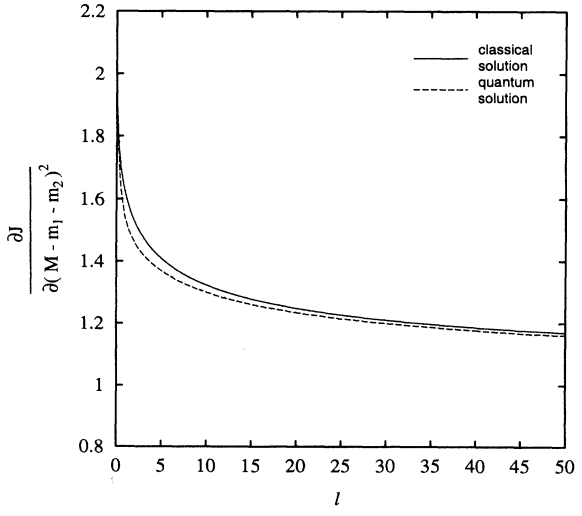

FIG. 2. Yrast solution (solid curve) compared to the quantum solution (dashed curve) for the displaced Regge slope with $m_1 = 0$ and $m_2 = 1.5$ GeV. We compare our solution for the same value of J (yrast) and l (quantum). In both cases the transition from heavy-light to light-light dynamics is clearly seen by the slope dropping from 2 to 1.

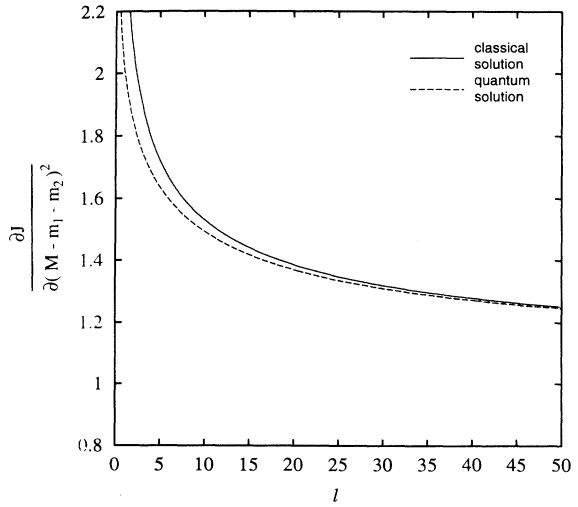

FIG. 3. Yrast solution (solid curve) compared to the quantum solution (dashed curve) for the displaced Regge slope with $m_1 = 0.5$ GeV and $m_2 = 1.5$ GeV. In this case we observe the transition from heavy-heavy dynamics at low l to light-light dynamics at large l.

light limit of (28). At large J where $m_2 < ar$ the slope approaches the Nambu limit (31). For $m_1 = 0.5$ GeV the solid curve of Fig. 3 illustrates the yrast-shifted Regge slope. At small J the heavy-heavy limit (25) is obtained, and for large J again the Nambu limit of unit slope is obtained. In both Figs. 2 and 3 the dashed curve is the quantum solution which will be discussed in Sec. IV. It should be noted that in each case the Regge behavior is most simply expressed in terms of the excitation energy $M - m_1 - m_2$.

III. QUANTIZATION OF THE CLASSICAL EQUATIONS

A. Equal-mass and the heavy-light case

The classical equations (1)–(8) for the equal-mass case reduce to

$$\frac{J}{r} = W_r \gamma_\perp v_\perp + arf(v_\perp) \ , \tag{32}$$

$$H = 2W_r\gamma_\perp + ar\frac{\arcsin v_\perp}{v_\perp} \ , \tag{33}$$

with

$$W_r = \sqrt{p_r^2 + m^2} \tag{34}$$

and

$$f(v_\perp) = \frac{1}{4v_\perp}\left(\frac{\arcsin v_\perp}{v_\perp} - \frac{1}{\gamma_\perp}\right) \ . \tag{35}$$

Since, in the limit of large quark masses [1, 3],

$$v_{\perp i} \to \frac{J}{m_i r} \ , \tag{36}$$

we have a good reason to believe that $v_{\perp_1}$ and $v_{\perp_2}$ should be Hermitian operators. Also, if we could invert the classical angular momentum equation for the equal-mass case (32), we would have

$$v_\perp = v_\perp(r, p_r^2, J) \ , \tag{37}$$

which means that $[v_\perp, r] \neq 0$ when $v_\perp$ and r are considered as quantum-mechanical operators. Therefore, the classical equations should be symmetrized and quantized as [1]

$$J \to \sqrt{l(l+1)}, \quad p_r^2 \to -\frac{1}{r}\frac{\partial^2}{\partial r^2}r \ , \tag{38}$$

$$2\frac{\sqrt{l(l+1)}}{r} = \{W_r, \gamma_\perp v_\perp\} + a\{r, f(v_\perp)\} \ , \tag{39}$$

$$H = \{W_r, \gamma_\perp\} + \frac{a}{2}\left\{r, \frac{\arcsin v_\perp}{v_\perp}\right\} \ , \tag{40}$$

where $\{A, B\} \equiv AB + BA$. Similarly, the heavy-light case classical equations with m_2 as the heavy quark mass,

$$\frac{J}{r} = W_r\gamma_\perp v_\perp + 2arf(v_\perp) \ , \tag{41}$$

$$H = m_2 + W_r\gamma_\perp + ar\frac{\arcsin v_\perp}{v_\perp} \ , \tag{42}$$

after quantization become

$$\frac{\sqrt{l(l+1)}}{r} = \frac{1}{2}\{W_r, \gamma_\perp v_\perp\} + a\{r, f(v_\perp)\} \ , \tag{43}$$

$$H = m_2 + \frac{1}{2}\{W_r, \gamma_\perp\} + \frac{a}{2}\left\{r, \frac{\arcsin v_\perp}{v_\perp}\right\} \ . \tag{44}$$

B. General case

In the general case with $m_1 \neq m_2$ things get more complicated, but proceed along similar lines. In addition to the equation defining the angular momentum, we also require that total momentum of the system must be zero, which is trivially satisfied in the two special cases considered above.

We begin by using the straight tube condition (8) and the quark separation variable (15) which give

$$r_i = \frac{v_{\perp_i}}{v_{\perp_1} + v_{\perp_2}} r \ , \qquad i = 1, 2 \ . \tag{45}$$

The classical RFT equations (1)–(7) can then be expressed in terms of $v_\perp$'s and r:

$$\frac{J}{r} = W_{r_1}\frac{\gamma_{\perp_1} v_{\perp_1}^2}{v_{\perp_1} + v_{\perp_2}} + W_{r_2}\frac{\gamma_{\perp_2} v_{\perp_2}^2}{v_{\perp_1} + v_{\perp_2}} + ar\frac{1}{(v_{\perp_1} + v_{\perp_2})^2}[\tilde{f}(v_{\perp_1}) + \tilde{f}(v_{\perp_2})] \ , \tag{46}$$

$$P_\perp = 0 = W_{r_1}\gamma_{\perp_1} v_{\perp_1} - W_{r_2}\gamma_{\perp_2} v_{\perp_2} - ar\frac{1}{v_{\perp_1} + v_{\perp_2}}\left(\frac{1}{\gamma_{\perp_1}} - \frac{1}{\gamma_{\perp_2}}\right) \ , \tag{47}$$

$$H = W_{r_1}\gamma_{\perp_1} + W_{r_2}\gamma_{\perp_2} + ar\frac{1}{v_{\perp_1} + v_{\perp_2}}(\arcsin v_{\perp_1} + \arcsin v_{\perp_2}) \ . \tag{48}$$

Here we have

$$W_{r_i} = \sqrt{p_r^2 + m_i^2} \ , \tag{49}$$

because of radial momentum conservation, and the function $\tilde{f}(v_\perp)$ is defined as

$$\tilde{f}(v_\perp) = \frac{1}{2}\left(\arcsin v_\perp - \frac{v_\perp}{\gamma_\perp}\right) = \frac{f(v_\perp)}{2v_\perp^2} \ . \tag{50}$$

If we could invert Eqs. (46) and (47) for $v_{\perp_1}$ and $v_{\perp_2}$, they would be in general different functions of r, p_r, and J, so that corresponding quantum-mechanical operators will not commute. Therefore, our quantized equations will contain products of three noncommuting factors, and we have to find the way to symmetrize them. In doing that, we have to keep in mind that our procedure must reduce to Eqs. (39) and (40) and (43) and (44) in the equal-mass and the heavy-light limits, respectively. The easiest way to ensure this is to symmetrize first between noncommuting factors containing $v_{\perp_1}$ and $v_{\perp_2}$ to obtain the symmetric operators $\hat{\mathcal{O}}(v_{\perp_1}, v_{\perp_2})$, and then to symmetrize between these operators and radial operators. If we do that, our quantized equations (46)–(48) become

$$\frac{\sqrt{l(l+1)}}{r} = \frac{1}{2}\left\{W_{r_1}, \frac{1}{2}\left\{\gamma_{\perp_1} v_{\perp_1}^2, \frac{1}{v_{\perp_1}+v_{\perp_2}}\right\}\right\} + \frac{1}{2}\left\{W_{r_2}, \frac{1}{2}\left\{\gamma_{\perp_2} v_{\perp_2}^2, \frac{1}{v_{\perp_1}+v_{\perp_2}}\right\}\right\}$$
$$+\frac{1}{2}a\left\{r, \frac{1}{2}\left\{\tilde{f}(v_{\perp_1})+\tilde{f}(v_{\perp_2}), \frac{1}{(v_{\perp_1}+v_{\perp_2})^2}\right\}\right\}, \tag{51}$$

$$P_\perp = 0 = \frac{1}{2}\{W_{r_1}, \gamma_{\perp_1} v_{\perp_1}\} - \frac{1}{2}\{W_{r_2}, \gamma_{\perp_2} v_{\perp_2}\} - \frac{a}{2}\left\{r, \frac{1}{2}\left\{\frac{1}{v_{\perp_1}+v_{\perp_2}}, \frac{1}{\gamma_{\perp_1}} - \frac{1}{\gamma_{\perp_2}}\right\}\right\}, \tag{52}$$

$$H = \frac{1}{2}\{W_{r_1}, \gamma_{\perp_1}\} + \frac{1}{2}\{W_{r_2}, \gamma_{\perp_2}\} + \frac{a}{2}\left\{r, \frac{1}{2}\left\{\frac{1}{v_{\perp_1}+v_{\perp_2}}, \arcsin v_{\perp_1} + \arcsin v_{\perp_2}\right\}\right\}. \tag{53}$$

IV. NUMERICAL SOLUTION OF THE QUANTIZED EQUATIONS

The RFT Hamiltonian (53) contains two unknown operators $v_{\perp_1}$ and $v_{\perp_2}$, which are in turn defined by Eqs. (51) and (52). If we introduce a complete set of basis states $\{e_k(\mathbf{r})\}$ and then truncate at a finite number N [13],

$$\psi(\mathbf{r}) \simeq \sum_{k=1}^{N} c_k e_k(\mathbf{r}), \tag{54}$$

these equations become two coupled transcendental $N \times N$ matrix equations involving unknown matrices of $v_{\perp_1}$ and $v_{\perp_2}$, and known r, $\frac{1}{r}$, and W_{r_i} matrices [4]. Our numerical solution for $v_{\perp_1}$ and $v_{\perp_2}$ is based on a simple $x = F(x)$ iteration algorithm applied to transcendental matrix equations.

Equation (51) can be written in the form

$$W_{r_1}\frac{1}{v_{\perp_1}+v_{\perp_2}}\gamma_{\perp_1} v_{\perp_1}^2 = 4\frac{\sqrt{l(l+1)}}{r} - W_{r_1}\gamma_{\perp_1} v_{\perp_1}^2 \frac{1}{v_{\perp_1}+v_{\perp_2}} - \left\{\gamma_{\perp_1} v_{\perp_1}^2, \frac{1}{v_{\perp_1}+v_{\perp_2}}\right\} W_{r_1}$$
$$-\left\{W_{r_2}, \left\{\gamma_{\perp_2} v_{\perp_2}^2, \frac{1}{v_{\perp_1}+v_{\perp_2}}\right\}\right\} - a\left\{r, \left\{\tilde{f}(v_{\perp_1})+\tilde{f}(v_{\perp_2}), \frac{1}{(v_{\perp_1}+v_{\perp_2})^2}\right\}\right\}. \tag{55}$$

If we multiply this equation by $v_{\perp_1}^{-1}\gamma_{\perp_1}^{-1}(v_{\perp_1}+v_{\perp_2})W_{r_1}^{-1}$ from the left, we get

$$v_{\perp_1} = v_{\perp_1}^{-1}\gamma_{\perp_1}^{-1}(v_{\perp_1}+v_{\perp_2})W_{r_1}^{-1}\left(4\frac{\sqrt{l(l+1)}}{r} - W_{r_1}\gamma_{\perp_1} v_{\perp_1}^2\frac{1}{v_{\perp_1}+v_{\perp_2}} - \left\{\gamma_{\perp_1} v_{\perp_1}^2, \frac{1}{v_{\perp_1}+v_{\perp_2}}\right\} W_{r_1}\right.$$
$$\left.-\left\{W_{r_2}, \left\{\gamma_{\perp_2} v_{\perp_2}^2, \frac{1}{v_{\perp_1}+v_{\perp_2}}\right\}\right\} - a\left\{r, \left\{\tilde{f}(v_{\perp_1})+\tilde{f}(v_{\perp_2}), \frac{1}{(v_{\perp_1}+v_{\perp_2})^2}\right\}\right\}\right). \tag{56}$$

We can do the same thing with Eq. (52) and obtain

$$v_{\perp_1} = \gamma_{\perp_1}^{-1}W_{r_1}^{-1}\left(-\gamma_{\perp_1} v_{\perp_1} W_{r_1} + \{W_{r_2}, \gamma_{\perp_2} v_{\perp_2}\}\right.$$
$$\left.+a\left\{r, \frac{1}{2}\left\{\frac{1}{v_{\perp_1}+v_{\perp_2}}, \frac{1}{\gamma_{\perp_1}} - \frac{1}{\gamma_{\perp_2}}\right\}\right\}\right). \tag{57}$$

For a successful iterative solution we must start with a good initial guess for matrices of $v_{\perp_1}$ and $v_{\perp_2}$. We then have initial guesses for matrices of all functions of these two operators and we can evaluate the right-hand sides of (56) and (57) as the new guesses for the $v_{\perp_1}$ matrix [let us call them $v_{\perp_1}(J)$ and $v_{\perp_1}(P_\perp)$]. Since we want to have both (51) and (52) satisfied simultaneously, we mix these two guesses with weights depending on the extent to which Eqs. (51) and (52) are satisfied, with the initial guesses for $v_{\perp_1}$ and $v_{\perp_2}$. For example, if Eq. (51) is satisfied twice as well as Eq. (52), then for the new guess for $v_{\perp_1}$ we take $\frac{1}{3}v_{\perp_1}(J) + \frac{2}{3}v_{\perp_1}(P_\perp)$. This ensures that both equations defining $v_{\perp_1}$ and $v_{\perp_2}$ will be simultaneously satisfied. Finally, since we are solving for matrices here, it is clear that our iteration scheme will be only marginally stable, and so we employ a relaxation procedure. For the final new guess for $v_{\perp_1}$ we take $(1-\eta)v_{\perp_1}(\text{old}) + \eta v_{\perp_1}(\text{new})$, where η is the small number (usually $\eta \leq 0.1$, and it becomes smaller if we increase number N of the basis states that we are working with). After we have found the new guess for $v_{\perp_1}$, we do the same thing for $v_{\perp_2}$, and keep iterating until we achieve the required precision.

Using the same procedure, we were able to solve for $v_\perp$

the equal-mass and the heavy-light case equations (39) and (43) even for as many as 50 basis states without too much effort and to achieve the very high accuracy of eight decimal places. The initial guess in these two cases is obtained by finding the $v_\perp$ from the nonsymmetrized angular momentum equations [4], and then symmetrizing it by taking the average of the nonsymmetric $v_\perp$ matrix and its transpose. The eigenvalues obtained from the symmetrized Hamiltonians (40) and (44) are usually lower by at most a few MeV's than the eigenvalues obtained from the nonsymmetrized equations. In Fig. 4 we compare the nonsymmetrized solution [4] for $m_1 = m_2 = 0$ (solid curve) with the symmetrized solution shown at integral angular momentum quantum number l. The difference between symmetrized and unsymmetrized solutions is at most a couple of MeV's over a wide range of rotational and radial excited states. With larger quark masses this difference decreases.

In the general case we have two unknown matrices and the equations are much more complicated. In addition, a good initial guess for $v_{\perp_1}$ and $v_{\perp_2}$ is not easy to find. Usually, for the initial guess for $v_{\perp_i}$ in the case of $l > 0$ (the $l = 0$ solution is trivial since $v_{\perp_1} = v_{\perp_2} = 0$) we use a symmetrized equal-mass guess for $m = m_i$ and the same angular momentum quantum number l. Despite these complications, for $N \leq 15$ basis states we have found that our procedure converges very quickly no matter how large the difference between m_2 and m_1 is (i.e., no matter how bad the initial guess is). In comparing with experimental data, we require only the lowest one or two eigenvalues, and these are determined within 10 MeV if we use five and within 1 MeV if we use ten basis states. Fits with $N = 10$ are reliable and completely adequate for our purposes.

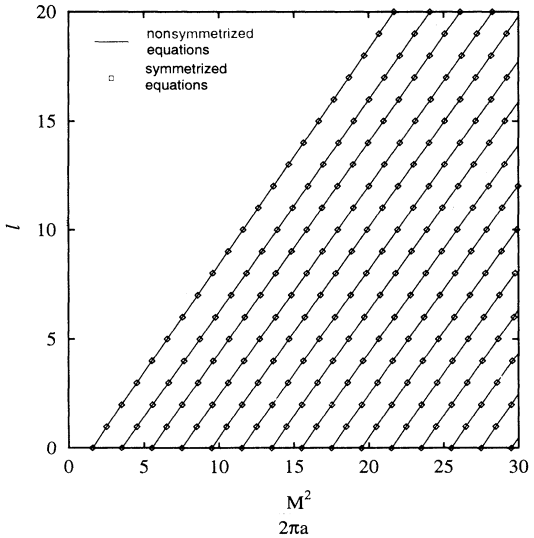

FIG. 4. Comparison of the symmetrized and nonsymmetrized equations for quark masses $m_1 = m_2 = 0$ with $N = 50$ basis states. The nonsymmetrized equations (32) and (33) discussed in [4] are found to agree with the fully symmetrized solutions of (39) and (40) to better than 5 MeV.

In Figs. 2 and 3 we compare the ground-state quantum solution (for continuous values of l [4]) with the classical yrast solution. We show in these figures the predicted shifted Regge slope. The correspondence limit at large angular momentum is well satisfied.

V. COMPARISON WITH EXPERIMENT

As mentioned earlier, mesons containing at least one heavy quark will have relatively small dependences on quark spins. It seems realistic then to compare our predictions, which do not include quark spin, directly to spin-averaged energy levels. There is, however, an additional feature which must be incorporated in the model to have a phenomenologically successful result.

A. Short-range interaction

The flux tube configuration has been assumed to dominate when the quarks are widely separated. At short distance there must be an attractive singular interaction due to single-gluon exchange. We parametrize the short and intermediate distance interactions by the usual potential

$$V_S(r) = -\frac{\kappa}{r} , \tag{58}$$

where at short distances $\kappa = \frac{4}{3}\alpha_s$. In the static limit the total potential then reduces to the well-known "Cornell potential" [14], a superposition of linear confinement $V_{\text{conf}} = ar$ and the Coulombic term (58). From general considerations we expect κ to "run" such that it will increase slowly as the quarks are separated (and hence the QCD scale decreases). In our comparison with the data we will allow different κ's for $c\bar{c}$, $b\bar{b}$, and the heavy-light mesons.

B. Constant term

A constant term is also added, yielding our model Hamiltonian

$$H = H_{\text{RFT}} + C - \frac{\kappa}{r} , \tag{59}$$

with H_{RFT} given by (53). The presence of the constant term does not change the model predictions but it does determine how the heavy quark masses change with the QCD scale.

C. Data and comparison with theory

We have used the quark model spectroscopic assignments and level masses of the Particle Data Group [15] to extract spin-averaged states for heavy-light mesons (Table I) and heavy-heavy mesons below the flavor threshold (Table II).

TABLE I. Heavy-light spin-averaged states. Spin-averaged masses are calculated in the usual way, by taking $\frac{3}{4}$ of the triplet and $\frac{1}{4}$ of the singlet mass.

State	Spectroscopic label J^P	$^{2S+1}L_J$	Spin-averaged mass (MeV)	Theory (MeV)	Error (MeV)
$c\bar{u}$, $c\bar{d}$ quarks					
D (1867)	0^-	$^1S_0$	$1S$ (1974)	1972	−2
D^* (2009)	1^-	$^3S_1$			
D_1 (2424)	1^+	$^1P_1$	$1P$ (2424)	2426	2
$c\bar{s}$ quarks					
D_s (1969)	0^-	$^1S_0$	$1S$ (2075)	2077	2
D_s^* (2110)	1^-	$^3S_1$			
D_{s_1} (2537)	1^+	$^1P_1$	$1P$ (2537)	2535	−2
$b\bar{u}$, $b\bar{d}$ quarks					
B (5279)	0^-	$^1S_0$	$1S$ (5312)	5313	1
B^* (5325)	1^-	$^3S_1$			
$b\bar{s}$ quarks					
B_s (5368)	0^-	$^1S_0$	$1S$ (5409)	5408	−1

From QCD one expects that the strong coupling constant and quark masses will become smaller as the QCD scale increases [16]. Since the energy scale for mesons is in the nonperturbative regime, one cannot expect that perturbative expressions for the running of α_s and quark masses agree quantitatively with the model results. However, one can expect qualitative agreement.

In order to show this, we have performed series of fits using the generalized RFT model equations, in which we have fixed the constant C in the Hamiltonian, the string tension a, and also the light quark mass $m_{u,d}$. The free parameters of the fits were $\kappa(hl)$, $m_s(hl)$, $m_c(hl)$, and $m_b(hl)$ for the heavy-light mesons, $\kappa(c\bar{c})$ and $m_c(c\bar{c})$ for the $c\bar{c}$ mesons, and $\kappa(b\bar{b})$ and $m_b(b\bar{b})$ for the $b\bar{b}$ mesons. As an illustration of the quality of our fits, in Tables I and II we present fits for the heavy-heavy and heavy-light mesons for $C = -0.8$ GeV, $a = 0.2$ GeV^2, and $m_{u,d} = 0.3$ GeV. The resulting values of the free fit parameters were

TABLE II. Heavy-heavy spin-averaged states. Since η_b's have not been observed yet, in calculating the spin-averaged mass for all S states in the $b\bar{b}$ system we assume $\Upsilon - \eta_b = 40 \pm 20$ MeV on the grounds that this splitting should be approximately one-third of the corresponding splitting in the $c\bar{c}$ systems. We estimate that the error introduced in this way is probably less than 5 MeV. We also assume that p-wave hyperfine splitting in the $b\bar{b}$ mesons is negligible.

State	Spectroscopic label J^P	$^{2S+1}L_J$	Spin-averaged mass (MeV)	Theory (MeV)	Error (MeV)
$c\bar{c}$ quarks					
η_c (2979)	0^-	$^1S_0$	$1S$ (3068)	3066	−2
ψ (3097)	1^-	$^3S_1$			
χ_{0c} (3415)	0^+	$^3P_0$	$1P$ (3525)	3519	−6
χ_{1c} (3511)	1^+	$^3P_1$			
χ_{2c} (3556)	2^+	$^3P_2$			
h_c (3525)	1^+	$^1P_1$			
η_c' (3594)	0^-	2^1S_0	$2S$ (3663)	3672	9
ψ' (3686)	1^-	2^3S_1			
$b\bar{b}$ quarks					
Υ (9460)	1^-	$^3S_1$	$1S$ (9450)	9451	1
Υ' (10023)	1^-	2^3S_1	$2S$ (10013)	10004	−9
Υ'' (10355)	1^-	3^3S_1	$3S$ (10345)	10349	4
χ_{0b} (9860)	0^+	$^3P_0$	$1P$ (9900)	9905	5
χ_{1b} (9892)	1^+	$^3P_1$			
χ_{2b} (9913)	2^+	$^3P_2$			
χ_{0b}' (10232)	0^+	2^3P_0	$2P$ (10261)	10260	−1
χ_{1b}' (10255)	1^+	2^3P_1			
χ_{2b}' (10268)	2^+	2^3P_2			

$$\left.\begin{array}{l} m_s = 0.487\ \text{GeV} \\ m_c = 1.955\ \text{GeV} \\ m_b = 5.391\ \text{GeV} \\ \kappa(hl) = 0.576 \end{array}\right] \quad hl \text{ mesons} ,$$

$$\left.\begin{array}{l} m_c = 1.816\ \text{GeV} \\ \kappa(c\bar{c}) = 0.532 \end{array}\right] \quad c\bar{c} \text{ mesons} , \tag{60}$$

$$\left.\begin{array}{l} m_b = 5.153\ \text{GeV} \\ \kappa(b\bar{b}) = 0.440 \end{array}\right] \quad b\bar{b} \text{ mesons} .$$

As one can see from Tables I and II, the fits are quite reasonable. All spin-averaged heavy-light states were reproduced to within 2 MeV, while heavy-heavy states had errors within 10 MeV.

To observe running in the RFT model, let us first consider the strong coupling constant $\kappa = \frac{4}{3}\alpha_s$. If we make the reasonable assumption that meson dynamics is governed roughly by the reduced mass of its constituent quarks, we expect that κ will decrease as we increase the light quark mass ($m_{u,d}$, m_s), and therefore the reduced mass. Furthermore, as we go from heavy-light to $c\bar{c}$ and then to $b\bar{b}$ mesons, the energy scale again increases, and the coupling constant should decrease. This behavior is exactly what we see in Fig. 5.

As far as m_c and m_b are concerned, first of all we expect larger heavy quark masses for $m_{u,d} = 0$, since the meson mass is roughly the sum of the masses of its constituents, and this is shown in Figs. 6 and 7 (two dashed lines). Furthermore, the constant C should just renormalize the heavy quark masses in the heavy-heavy systems ($m_i \to m_i + \frac{1}{2}C$). From our fits we find (solid lines in Figs. 6 and 7)

$$m_c(C) = 1.368\ \text{GeV} - 0.560C \quad (c\bar{c} \text{ mesons}) , \tag{61}$$

$$m_b(C) = 4.739\ \text{GeV} - 0.520C \quad (b\bar{b} \text{ mesons}) , \tag{62}$$

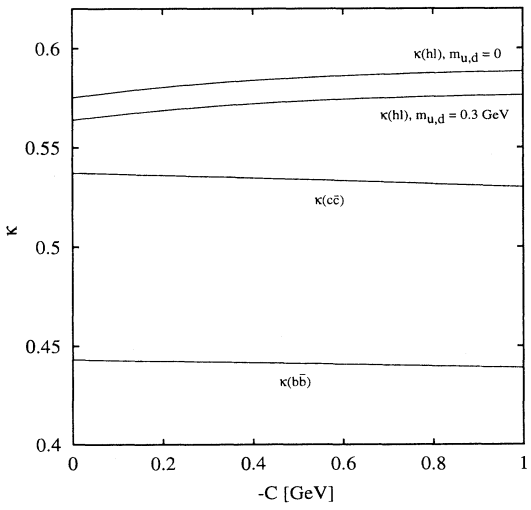

FIG. 5. Strong coupling constant as a function of C in the heavy-light (for $m_{u,d} = 0$ and $m_{u,d} = 0.3$ GeV) $c\bar{c}$ and $b\bar{b}$ mesons. The values of κ found are roughly independent of C, but systematically fall with the running QCD scale (reduced mass).

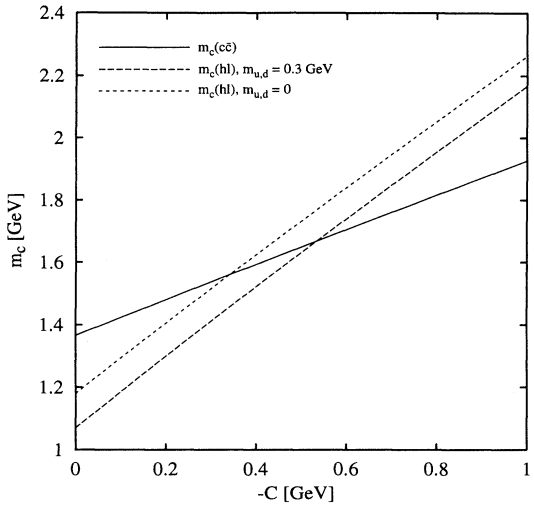

FIG. 6. Mass of the c quark as a function of C in the heavy-light (for $m_{u,d} = 0$ and $m_{u,d} = 0.3$ GeV, dashed lines) and $c\bar{c}$ mesons. For C less than about -0.5 GeV, m_c falls with an increasing QCD scale (reduced mass).

as expected. For the heavy-light systems, one might expect that we have $m_i \to m_i + C$, since we have kept the light quark masses fixed. For $m_{u,d} = 0.3$ GeV our fits give (dashed lines in Figs. 6 and 7)

$$m_c(C) = 1.078\ \text{GeV} - 1.094C , \tag{63}$$

$$m_b(C) = 4.571\ \text{GeV} - 1.025C , \tag{64}$$

and for $m_{u,d} = 0$ we find

$$m_c(C) = 1.188\ \text{GeV} - 1.081C , \tag{65}$$

$$m_b(C) = 4.660\ \text{GeV} - 1.024C . \tag{66}$$

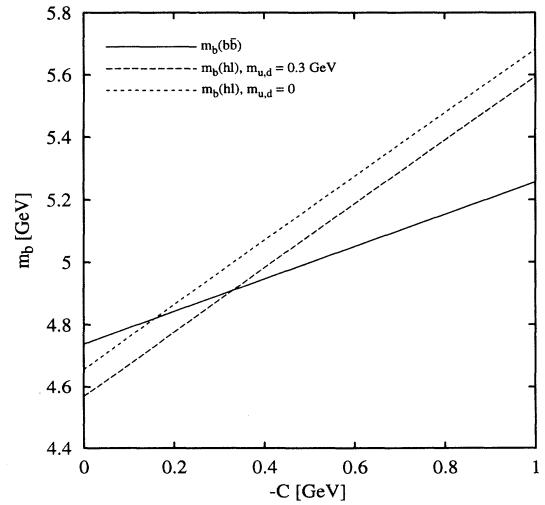

FIG. 7. Mass of the b quark as a function of C in the heavy-light (for $m_{u,d} = 0$ and $m_{u,d} = 0.3$ GeV, dashed lines) and $b\bar{b}$ mesons. For C less than about -0.3 GeV, m_c falls with an increasing QCD scale (reduced mass).

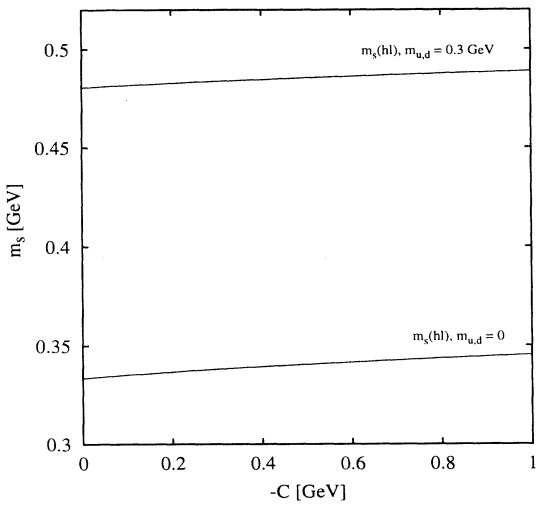

FIG. 8. Mass of the s quark as a function of C in the heavy-light (for $m_{u,d} = 0$ and $m_{u,d} = 0.3$ GeV) mesons.

Also, as stated before, one would expect that heavy quark masses should decrease as we go from the heavy-light to the heavy-heavy systems. As we can see from Figs. 6 and 7, this is satisfied only for large negative values of C. This gives us an estimate of the upper limit for its possible values. In particular, C must be more negative than about -0.5 GeV for both m_c and m_b to run in a generally accepted manner.

Finally, from Fig. 8 one can see that the strange quark mass (obtained from the heavy-light fits) is almost independent of C.

VI. CONCLUSIONS

In this paper we have discussed the relativistic flux tube model with arbitrary mass spinless quarks on its ends. We have obtained the classical rotational solution (yrast). The quantum solution is also proposed and solved numerically. In both the classical and quantized solutions an important ingredient is the condition of a fixed center of momentum. The quantum solution also involved a careful treatment of symmetrization of the equations of motion. We have confined our comparison of the RFT with data to mesons containing at least one heavy quark primarily because in this case spin dependence should be small enough that the spin-averaged data can be compared to our spinless quark calculation. We have done a simultaneous fit to all of the available heavy-light and heavy-heavy data, and we have obtained an excellent fit to the spin-averaged levels. To achieve this agreement we have allowed the short-range coupling constant κ and the heavy quark masses m_c and m_b to run with the QCD scale. We note that κ always decreases with increasing scale (reduced mass), and that the heavy quark masses decrease with increasing scale if the constant C is more negative than roughly -0.5 GeV.

It will be important to include spin in our model. Fortunately the orbital angular momentum discussion in this paper will form a key ingredient of the more complete calculation. The results will be somewhat different even for the spin-averaged case since a Darwin-type term will arise due to the fermionic nature of the quarks at both long and short ranges. The RFT model formulation with fermionic quarks was discussed in some detail [3] previously.

ACKNOWLEDGMENTS

We would like to thank Collin Olson and Paul Stevenson for helpful discussions. This work was supported in part by the U.S. Department of Energy under Contract No. DE-AC02-76ER00881 and in part by the University of Wisconsin Research Commitee with funds granted by the Wisconsin Alumni Research Foundation.

[1] Dan LaCourse and M. G. Olsson, Phys. Rev. D **39**, 2751 (1989).
[2] Collin Olson, M. G. Olsson, and Ken Williams, Phys. Rev. D **45**, 4307 (1992).
[3] M. G. Olsson and Ken Williams, Phys. Rev. D **48**, 417 (1993).
[4] C. Olson, M. G. Olsson, and D. LaCourse, Phys. Rev. D **49**, 4675 (1994).
[5] E. Eichten and F. Feinberg, Phys. Rev. D **23**, 2724 (1981); D. Gromes, Z. Phys. C **22**, 265 (1984); **26**, 401 (1984); A. Barchielli, E. Montaldi, and G. M. Prosperi, Nucl. Phys. **B296**, 625 (1988); **B303**, 752(E) (1988).
[6] A. Barchielli, N. Brambilla, and G. M. Prosperi, Nuovo Cimento **103A**, 59 (1989).
[7] N. Brambilla and G. M. Prosperi, Phys. Lett. B **236**, 69 (1990).
[8] W. Buchmüller, Phys. Lett. **112B**, 479 (1982).
[9] Robert D. Pisarski and John D. Stack, Nucl. Phys. **B286**, 657 (1987).
[10] A. Yu. Dubin, A. B. Kaidalov, and Yu. A. Simonov, Phys. Atom. Nucl. **56**, 1745 (1993); Phys. Lett. B **323**, 41 (1994).
[11] E. E. Salpeter, Phys. Rev. **87**, 328 (1952).
[12] Alan Chodos and Charles B. Thorn, Nucl. Phys. **B72**, 509 (1974); M. Ida, Prog. Theor. Phys. **59**, 1661 (1978).
[13] A discussion of the Galerkin method and the definition of the specific basis states used here is found in S. Jacobs, M. G. Olsson, and C. J. Suchyta III, Phys. Rev. D **33**, 3338 (1986).
[14] T. Appelquist, R. M. Barnett, and K. D. Lane, Annu. Rev. Nucl. Part. Sci. **28**, 38 (1978).
[15] Particle Data Group, L. Montanet *et al.*, Phys. Rev. D **50**, 1320 (1994).
[16] H. Georgi and H. D. Politzer, Phys. Rev. D **14**, 1829 (1976).